

RESEARCH ARTICLE

Improved algorithm for analytical solution of the heat conduction problem in doubly periodic 2D composite materials

D. Kapanadze^a, G. Mishuris^b and E. Pesetskaya^{a*}

^a*A. Razmadze Mathematical Institute, Tbilisi State University, Georgia;* ^b*Institute of Mathematics and Physics, Aberystwyth University, UK*

(August 2013)

We consider a boundary value problem (BVP) in unbounded 2D doubly periodic composite with circular inclusions having arbitrary constant conductivities. By introducing complex potentials, the BVP for the Laplace equation is transformed to a special R -linear BVP for doubly periodic analytic functions. This problem is solved with use of the method of functional equations. The R -linear BVP is transformed to a system of functional equations. A new improved algorithm for solution of the system is proposed. It allows one not only to compute the average property but to reconstruct the solution components (temperature and flux) at an arbitrary point of the composite. Several computational examples are discussed in details demonstrating high efficiency of the method. Indirect estimate of the algorithm accuracy has been also provided.

Keywords: 2D unbounded composite material, steady-state conductivity problem, effective conductivity, functional equations, temprature/flux distribution

AMS Subject Classification: 30E25, 35B27, 74Q05, 33E05

1. Introduction

Heterogeneous media model problems serve the purposes of material science studies for the analysis of the various fields and prediction of their properties [1–4]. Different approaches for study linear inhomogeneous material are presented in well-known monographs [5–10]. One of the approaches dealing with composite materials is the so-called homogenization method (see [11, 12]). Mathematical aspects of the higher order homogenization have been developed in [13]. The limiting case for large (close to the maximal value) rectangular cross-section cylindrical cavities by means of an asymptotic procedure were studied in [11] where explicit analytical expressions for effective parameters have been also found. Non-local phenomena resulting from a high contrast (or anisotropy) of composite structures were studied in [5, 14]. In two- and three-dimensional cases the Rayleigh multipole expansions method and its generalizations is effectively used (see, e.g.[10, 15]). Various analytical approaches have been discussed in [16, 17].

Essential progress has been already achieved in the area of numerical analysis of composite material properties. Such approach is naturally restricted to a finite cell (or a few cell - representative element) size in order to reduce the computation cost. A vast literature related to this approach can be found in [18]. The major

*Corresponding author. Email: kate.pesetskaya@gmail.com

advantage of analytical approach is a possibility to describe and analyze the material properties by means of explicit analytical formulas. This allow one to reveal an influence of the materials characteristics (like size, shape, location of components, their material properties) on the overall properties of the composite (homogeneous approach) [1, 19–24]. Recently, the relationship between the effective properties in the problem of the heat conduction and elasticity have been revealed and effectively exploited [25, 26].

In this paper, we reveal another advantage of the analytical approach showing that it is capable to efficiently reconstruct the global and local distributions of the physical fields. We consider well-known linear heat conduction problem in 2D unbounded doubly periodic composite with material properties independent of the temperature field. The components (inclusions) are supposed to be disjoint disks formed a doubly periodic structure. We consider the steady process governed here by the Laplace equation. We will mostly follow by pioneering work [1], but a few important improvements will be introduced. First, we slightly change the problem formulation introducing more natural conditions at infinity prescribing only average flux, at an arbitrary direction, in contrast to the problem investigated in [1], where a special temperature distribution assumed in the direction of the coordinate system. In the linear formulation, our approach is in fact equivalent to periodic conditions for flux on the boundary of the minimal representative cell.

Although, we treat the problem using the methods developed in [1], reducing the corresponding BVP to a system of functional equations with respect to doubly periodic analytical functions, we substantially change the algorithm for the numerical calculations. The algorithm in [1] is mostly oriented to find the effective conductivity. In this case, it is sufficient to know values of the heat flux in the centers of inclusions only. However, it turns out that it may not guarantee the best accuracy when defining values of the flux outside the inclusion or reconstructing the temperature distribution. Modified algorithm presented in this work allows one to increase an accuracy of the numerical computations an any point in the distance from the centers of inclusions and to find the temperature field (with accuracy to an arbitrary constant). The proposed modification allows us to find the flux distribution in an explicit form containing all parameters of the considered model such as conductivities of the matrix and inclusions, radii and centers of inclusions, an intensity and an angle of the flux. As the previous algorithm, it also relays on the values of special Eisenstein functions ([27]).

The paper is organized as follows. In Section 2 we describe the geometry of the considered composites and formulate the mathematical problem basing on proper physical assumptions. In Section 3 we briefly overview the auxiliary problem stated in [1], show a connection with the original problem.

In Section 4 we describe a new algorithm in details and show that both components of the solution, the flux and the temperature, can be computed in the unique scheme. Finally, numerical calculations are performed and discussed in Section 5 to demonstrate algorithm accuracy, robustness and effectiveness.

2. Statement of the problem

We consider a lattice L which is defined by the two fundamental translation vectors “1” and “ i ” (where $i^2 = -1$) in the complex plane $\mathbb{C} \cong \mathbb{R}^2$ (with the standard notation $z = x + iy$).

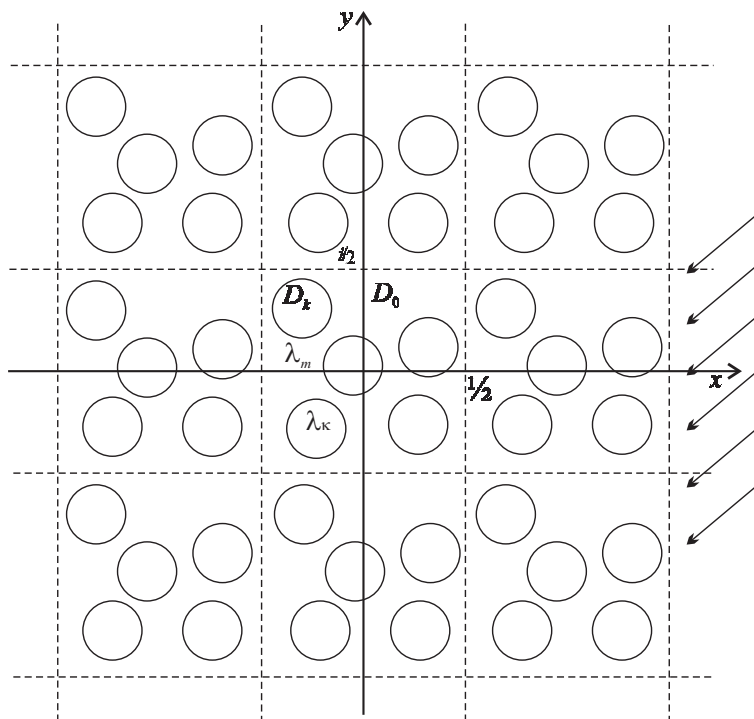


Figure 1. The representative cell $Q_{(0,0)}$ within doubly periodic composite.

Here, the representative cell (see Figure 1) will be the square

$$Q_{(0,0)} := \left\{ z = t_1 + it_2 \in \mathbb{C} : -\frac{1}{2} < t_p < \frac{1}{2}, p = 1, 2 \right\}. \quad (1)$$

Let $\mathcal{E} := \bigcup_{m_1, m_2} \{m_1 + im_2\}$ be the set of the lattice points, where $m_1, m_2 \in \mathbb{Z}$. The cells corresponding to the points of the lattice \mathcal{E} will be denoted by

$$Q_{(m_1, m_2)} = Q_{(0,0)} + m_1 + im_2 := \{z \in \mathbb{C} : z - m_1 - im_2 \in Q_{(0,0)}\}. \quad (2)$$

It is considered the situation when mutually disjoint disks (inclusions) $D_k := \{z \in \mathbb{C} : |z - a_k| < r_k\}$ with different radii r_k and boundaries $\partial D_k := \{z \in \mathbb{C} : |z - a_k| = r_k\}$ ($k = 1, 2, \dots, N$) are located inside the cell $Q_{(0,0)}$ and periodically repeated in all cells $Q_{(m_1, m_2)}$. Let us denote by

$$D_0 := Q_{(0,0)} \setminus \left(\bigcup_{k=1}^N D_k \cup \partial D_k \right) \quad (3)$$

the connected domain obtained by removing of the inclusions from the cell $Q_{(0,0)}$ (cf. Figure 1).

Let us consider the problem of determination of the heat flux function of a doubly periodic composite material with matrix

$$D_{matrix} = \bigcup_{m_1, m_2} ((D_0 \cup \partial Q_{(0,0)}) + m_1 + im_2) \quad (4)$$

and inclusions

$$D_{inc} = \bigcup_{m_1, m_2} \bigcup_{k=1}^N (D_k + m_1 + im_2) \quad (5)$$

occupied by materials of conductivities $\lambda_m > 0$ and $\lambda_k > 0$ ($k = 1, \dots, N$), respectively. For this purpose, we consider a problem of the determination of the potential of the corresponding fields, i.e., a temperature function $T = T(x, y)$ satisfying the Laplace equation in each component of the composite material

$$\Delta T(z) = 0, \quad z \in D_{matrix} \cup D_{inc}, \quad (6)$$

which have to satisfy the following boundary conditions on all ∂D_k , $k = 1, 2, \dots, N$:

$$T(t) = T_k(t), \quad (7)$$

$$\lambda_m \frac{\partial T}{\partial n}(t) = \lambda_k \frac{\partial T_k}{\partial n}(t), \quad t \in \bigcup_{m_1, m_2} \partial D_k. \quad (8)$$

Here, the vector $n = (n_1, n_2)$ is the outward unit normal vector to ∂D_k , $\frac{\partial}{\partial n} = n_1 \frac{\partial}{\partial x} + n_2 \frac{\partial}{\partial y}$ is the outward normal derivative, and

$$T(t) := \lim_{z \rightarrow t, z \in D_0} T(z), \quad T_k(t) := \lim_{z \rightarrow t, z \in D_k} T(z). \quad (9)$$

The conditions (7)–(8) form the so-called *ideal (perfect) contact conditions*.

The thermal loading for the composite is described weakly by the flux given at infinity or more accurately by its intensity A . We assume that the flux is directed θ which does not coincide, in general, with the orientation of the periodic cell (see, Figure 1). According to the conservation law and the ideal contact condition between the different materials, the flux is continuous in the entire structure. Moreover, as a result of such formulation, the temperature, which is also continuous as the results of the ideal transmission conditions along the interface between the matrix and inclusions, possesses non-zero jumps across any cell.

In addition, we assume that the heat flux is periodic on y . Thus,

$$\lambda_m T_y \left(x, \frac{1}{2} \right) = \lambda_m T_y \left(x, -\frac{1}{2} \right) = -A \sin \theta + q_1(x), \quad (10)$$

where A is the intensity of an external flux. The heat flux is periodic on x , consequently,

$$\lambda_m T_x \left(-\frac{1}{2}, y \right) = \lambda_m T_x \left(\frac{1}{2}, y \right) = -A \cos \theta + q_2(y). \quad (11)$$

To complement to the average flux conditions at infinity, the latter immediately proves that the equalities

$$\int_{-1/2}^{1/2} q_j(\xi) d\xi = 0 \quad (12)$$

are valid for the unknown functions q_j , ($j = 1, 2$). As a result of (10) and (11), the heat flux has a zero mean value along the cell

$$\int_{\partial Q_{(m_1, m_2)}} \frac{\partial T(s)}{\partial n} ds = 0. \quad (13)$$

From the physics point of view, condition (13) is the consequence of the fact that no source (sink) exists in the cells. Moreover, since there is no source (sink) inside the composite, i.e., neither in the matrix of the composite, nor in any inclusion (the total heat flux through any closed simply connected curve is equal to zero), we have

$$\int_{\partial D_{k+m_1+im_2}} \frac{\partial T}{\partial n} ds = 0. \quad (14)$$

We will introduce complex potentials $\varphi(z)$ and $\varphi_k(z)$ which are analytic in D_0 and D_k , and continuously differentiable in the closures of D_0 and D_k , respectively, by using the following relations

$$T(z) = \begin{cases} \operatorname{Re}(\varphi(z) + Bz), & z \in D_{matrix}, \\ \frac{2\lambda_m}{\lambda_m + \lambda_k} \operatorname{Re} \varphi_k(z), & z \in D_{inc}, \end{cases} \quad (15)$$

where B is an unknown constant belong to \mathbb{C} . Besides, we assume the the real part of φ is doubly periodic in D_0 , i.e.

$$\operatorname{Re} \varphi(z + 1) - \operatorname{Re} \varphi(z) = 0, \quad \operatorname{Re} \varphi(z + i) - \operatorname{Re} \varphi(z) = 0.$$

Note that in general the imaginary part of φ is not doubly periodic in D_0 .

Let us show that φ is single-valued function in D_{matrix} . We take a harmonic function v in D_{matrix} which is the harmonic conjugate to T . For this pair of functions the Cauchy-Riemann equations $\frac{\partial T}{\partial x} = \frac{\partial v}{\partial y}$, $\frac{\partial T}{\partial y} = -\frac{\partial v}{\partial x}$ (or the so called normal-tangent Cauchy-Riemann equations $\frac{\partial T}{\partial n} = \frac{\partial v}{\partial s}$, $\frac{\partial T}{\partial s} = -\frac{\partial v}{\partial n}$) have to be valid. The functions v has the following form:

$$v(z) = \begin{cases} \operatorname{Im}(\varphi(z) + Bz), & z \in D_{matrix}, \\ \frac{2\lambda_m}{\lambda_m + \lambda_k} \operatorname{Im} \varphi_k(z), & z \in D_{inc}, \end{cases} \quad (16)$$

with the same unknown constant B .

As it follows from (13) – (14) we can write

$$\int_{\partial Q_{(m_1, m_2)}} \frac{\partial v}{\partial s} ds = 0, \quad \int_{\partial D_{k+m_1+im_2}} \frac{\partial v}{\partial s} ds = 0. \quad (17)$$

These relations yield that the harmonic function v is single-valued in the domain D_{matrix} . Therefore, the complex potential $\varphi(z)$ is single-valued in D_{matrix} .

To determine the flux $\nabla T(x, y)$, we need to obtain derivatives of the complex potentials:

$$\begin{aligned}\psi(z) &:= \frac{\partial \varphi}{\partial z} = \frac{\partial T}{\partial x} - i \frac{\partial T}{\partial y} - B, & z \in D_0, \\ \psi_k(z) &:= \frac{\partial \varphi_k}{\partial z} = \frac{\lambda_m + \lambda_k}{2\lambda_m} \left(\frac{\partial T_k}{\partial x} - i \frac{\partial T_k}{\partial y} \right), & z \in D_k.\end{aligned}\tag{18}$$

Let us rewrite conditions (7)–(8) in terms of the complex potentials $\varphi(z)$ and $\varphi_k(z)$. Let s be the natural parameter of the curve ∂D_k and

$$\frac{\partial}{\partial s} = -n_2 \frac{\partial}{\partial x} + n_1 \frac{\partial}{\partial y}\tag{19}$$

be the tangent derivative along ∂D_k . Applying the Cauchy-Riemann equations, the equality (8) can be written as

$$\lambda_m \frac{\partial v}{\partial s}(t) = \lambda_k \frac{\partial v_k}{\partial s}(t), \quad |t - a_k| = r_k.\tag{20}$$

Integrating the last equality on s , we arrive at the relation

$$\lambda_m v(t) = \lambda_k v_k(t) + c,\tag{21}$$

where c is an arbitrary constant. We put $c = 0$ since the imaginary part of the function φ is determined up to an additive constant which does not impact on the form of T . Using (16), we have

$$\operatorname{Im} \varphi(t) = -\operatorname{Im}(Bt) + \frac{2\lambda_k}{\lambda_m + \lambda_k} \operatorname{Im} \varphi_k(t), \quad |t - a_k| = r_k.\tag{22}$$

Using (15), we are able to write the equality (7) in the following form:

$$\operatorname{Re} \varphi(t) = -\operatorname{Re}(Bt) + \frac{2\lambda_m}{\lambda_m + \lambda_k} \operatorname{Re} \varphi_k.\tag{23}$$

Adding the relation (23) and (22) multiplied by i , and using $\operatorname{Re} \varphi_k = \frac{\varphi_k + \overline{\varphi_k}}{2}$, $\operatorname{Im} \varphi_k = \frac{\varphi_k - \overline{\varphi_k}}{2i}$, $t - a_k = \frac{r_k^2}{t - a_k}$, we have

$$\varphi(t) = \varphi_k(t) - \overline{\rho_k \varphi_k(t)} - Bt, \quad |t - a_k| = r_k,\tag{24}$$

where $\rho_k = \frac{\lambda_k - \lambda_m}{\lambda_k + \lambda_m}$.

Let us now differentiate (24). First, note that

$$[\overline{\varphi(t)}]' = - \left(\frac{r_k}{t - a_k} \right)^2 \overline{\varphi'(t)}, \quad |t - a_k| = r_k.\tag{25}$$

This can be easily shown by representing the function φ in the form $\varphi(z) = \sum_{l=0}^{\infty} \alpha_k (z - a_k)^l$, $|z - a_k| \leq r_k$, and by using the relation $t = \frac{r_k^2}{t - a_k} + a_k$ on the boundary $|t - a_k| = r_k$. Thus, after differentiating (24) and using (18), we arrive

at the following \mathbb{R} -linear conjugation problem ([16]) on each contour $|t - a_k| = r_k$,

$$\psi(t) = \psi_k(t) + \rho_k \left(\frac{r_k}{t - a_k} \right)^2 \overline{\psi_k(t)} - B, \quad (26)$$

with $k = 1, 2, \dots, N$.

Remark 2.1. Thus, the boundary value problem (6)-(8), (10)-(11) for harmonic functions is reduced to \mathbb{R} -linear conjugation problem (26) for analytical doubly periodic functions $\psi, \psi_1, \dots, \psi_N$.

We will seek a solution $\psi(z), \psi_k(z)$ of the problem (26) as a sum $\psi(z) = \psi^{(1)}(z) + \psi^{(2)}(z)$, $\psi_k(z) = \psi_k^{(1)}(z) + \psi_k^{(2)}(z)$ of solutions of the following two BVPs:

$$\psi^{(1)}(t) = \psi_k^{(1)}(t) + \rho_k \left(\frac{r_k}{t - a_k} \right)^2 \overline{\psi_k^{(1)}(t)} - B_1, \quad (27)$$

$$\psi^{(2)}(t) = \psi_k^{(2)}(t) + \rho_k \left(\frac{r_k}{t - a_k} \right)^2 \overline{\psi_k^{(2)}(t)} - \iota B_2, \quad (28)$$

where $\psi_k^{(1)}$ and $\psi_k^{(2)}$ are analytical doubly periodic functions, $B = B_1 + \iota B_2$.

3. Formulation of an auxiliary problem

In this section we briefly overview the auxiliary problem discussed in [1] and represent necessary results in convenient for us form. Let \tilde{T} be a solution of the boundary value problem (6)-(8) with a constant jump corresponding to the external field applied in the x -direction

$$\tilde{T}(z + 1) = \tilde{T}(z) + 1, \quad \tilde{T}(z + \iota) = \tilde{T}(z). \quad (29)$$

The complex potentials $\tilde{\varphi}^{(1)}(z)$ and $\tilde{\varphi}_k^{(1)}(z)$ are introduced as follows

$$\tilde{T}(z) = \begin{cases} \operatorname{Re}(\tilde{\varphi}^{(1)}(z) + z), & z \in D_{\text{matrix}}, \\ \frac{2\lambda_m}{\lambda_m + \lambda_k} \operatorname{Re} \tilde{\varphi}_k^{(1)}(z), & z \in D_{\text{inc}}. \end{cases} \quad (30)$$

Note that $\tilde{\varphi}^{(1)}(z)$ and $\tilde{\varphi}_k^{(1)}(z)$ are analytic in D_0 and D_k , and continuously differentiable in the closures of D_0 and D_k , respectively. Besides, the real part of $\tilde{\varphi}^{(1)}$ is doubly periodic in D_0 , i.e.

$$\operatorname{Re} \tilde{\varphi}^{(1)}(z + 1) - \operatorname{Re} \tilde{\varphi}^{(1)}(z) = 0, \quad \operatorname{Re} \tilde{\varphi}^{(1)}(z + \iota) - \operatorname{Re} \tilde{\varphi}^{(1)}(z) = 0. \quad (31)$$

In general, the imaginary part of $\tilde{\varphi}^{(1)}$ is not doubly periodic in D_0 . It turns out that they satisfy the following \mathbb{R} -linear conjugation boundary value problem obtained in [1]:

$$\tilde{\varphi}^{(1)}(t) = \tilde{\varphi}_k^{(1)}(t) - \overline{\rho_k \tilde{\varphi}_k^{(1)}(t)} - t, \quad |t - a_k| = r_k. \quad (32)$$

Differentiating the last equality, we obtain that the boundary value problem (6)-(8), (29) is reduced to the \mathbb{R} -linear conjugation boundary value problem for analytical doubly periodic functions $\tilde{\psi}^{(1)}, \tilde{\psi}_1^{(1)}, \dots, \tilde{\psi}_N^{(1)}$ (cf. [1]):

$$\tilde{\psi}^{(1)}(t) = \tilde{\psi}_k^{(1)}(t) + \rho_k \left(\frac{r_k}{t - a_k} \right)^2 \overline{\tilde{\psi}_k^{(1)}(t)} - 1 \quad (33)$$

with

$$\frac{\partial \tilde{T}}{\partial x} - \iota \frac{\partial \tilde{T}}{\partial y} = \begin{cases} \tilde{\psi}^{(1)}(z) + 1, & z \in D_{matrix}, \\ \frac{2\lambda_m}{\lambda_m + \lambda_k} \tilde{\psi}_k^{(1)}(z), & z \in D_{inc}, \end{cases} \quad (34)$$

and

$$\begin{aligned} \tilde{\psi}^{(1)}(z) &:= \frac{\partial \tilde{\varphi}^{(1)}}{\partial z} = \frac{\partial \tilde{T}}{\partial x} - \iota \frac{\partial \tilde{T}}{\partial y} - 1, & z \in D_0, \\ \tilde{\psi}_k^{(1)}(z) &:= \frac{\partial \tilde{\varphi}_k^{(1)}}{\partial z} = \frac{\lambda_m + \lambda_k}{2\lambda_m} \left(\frac{\partial \tilde{T}_k}{\partial x} - \iota \frac{\partial \tilde{T}_k}{\partial y} \right), & z \in D_k. \end{aligned} \quad (35)$$

Besides, we mention that when the temperature has a constant jump corresponding to the external field applied in the y -direction

$$\tilde{T}(z + 1) = \tilde{T}(z), \quad \tilde{T}(z + \iota) = \tilde{T}(z) - 1,$$

the temperature is defined as

$$\tilde{T}(z) = \begin{cases} \operatorname{Re}(\tilde{\varphi}^{(2)}(z) + \iota z), & z \in D_{matrix}, \\ \frac{2\lambda_m}{\lambda_m + \lambda_k} \operatorname{Re} \tilde{\varphi}_k^{(2)}(z), & z \in D_{inc}, \end{cases} \quad (36)$$

with corresponding functions $\tilde{\varphi}^{(2)}, \tilde{\varphi}_k^{(2)}$ possess the same properties as the functions $\tilde{\varphi}^{(1)}, \tilde{\varphi}_k^{(1)}$, and

$$\tilde{\varphi}^{(2)}(t) = \tilde{\varphi}_k^{(2)}(t) - \rho_k \overline{\tilde{\varphi}_k^{(2)}(t)} - \iota t, \quad |t - a_k| = r_k.$$

The corresponding \mathbb{R} -linear conjugation boundary value problem has a form

$$\tilde{\psi}^{(2)}(t) = \tilde{\psi}_k^{(2)}(t) + \rho_k \left(\frac{r_k}{t - a_k} \right)^2 \overline{\tilde{\psi}_k^{(2)}(t)} - \iota, \quad |t - a_k| = r_k. \quad (37)$$

The problems (27) and (28) can be reduced to the problems (33) and (37) by the following replacements:

$$\psi^{(1)}(z) = B_1 \tilde{\psi}^{(1)}(z), \quad \psi_k^{(1)}(z) = B_1 \tilde{\psi}_k^{(1)}(z), \quad (38)$$

$$\psi^{(2)}(z) = B_2 \tilde{\psi}^{(2)}(z), \quad \psi_k^{(2)}(z) = B_2 \tilde{\psi}_k^{(2)}(z). \quad (39)$$

Remark 3.1. It is easy to verify that the functions $\tilde{\psi}^\perp(z) := \imath\tilde{\psi}^{(2)}(\imath z)$ and $\tilde{\psi}_k^\perp(z) := \imath\tilde{\psi}_k^{(2)}(\imath z)$ satisfy the following \mathbb{R} -linear conjugation boundary value problem

$$\tilde{\psi}^\perp(t) = \tilde{\psi}_k^\perp(t) + \rho_k \left(\frac{r_k}{t - b_k} \right)^2 \overline{\tilde{\psi}_k^\perp(t)} + 1, \quad |t - b_k| = r_k, \quad b_k = -\imath a_k. \quad (40)$$

Note that $\tilde{\psi}^{(2)}(z) = -\imath\tilde{\psi}^\perp(-\imath z)$ and $\tilde{\psi}_k^{(2)}(z) = -\imath\tilde{\psi}_k^\perp(-\imath z)$.

Thus, to find a solution of the problem (26), it is sufficient to find solutions $\tilde{\psi}^{(1)}(z)$, $\tilde{\psi}_k^{(1)}(z)$ and $\tilde{\psi}^\perp(z)$, $\tilde{\psi}_k^\perp(z)$ of the problems (33) and (40), respectively.

4. Solution of the problem

First, let us find the real constants B_1 and B_2 .

We introduce further notations

$$I := \int_{-\frac{1}{2}}^{\frac{1}{2}} \operatorname{Re} \tilde{\psi}^{(1)}\left(\frac{1}{2} + \imath y\right) dy, \quad I^\perp := \int_{-\frac{1}{2}}^{\frac{1}{2}} \operatorname{Re} \tilde{\psi}^\perp\left(\frac{1}{2} + \imath y\right) dy.$$

In general, the integrals I and I^\perp differ from zero. As it is shown in Remark 4.3 below

$$\int_{-\frac{1}{2}}^{\frac{1}{2}} \operatorname{Im} \tilde{\psi}^{(1)}\left(x + \frac{\imath}{2}\right) dx = 0. \quad (41)$$

Taking $B_2 = 0$ (which corresponds to the problem (27)) and using (15), (18) and (38), we obtain

$$\lambda_m \frac{\partial T(x, \frac{1}{2})}{\partial y} = -\lambda_m \operatorname{Im} \left(\psi\left(x + \frac{\imath}{2}\right) + B \right) = -\lambda_m B_1 \operatorname{Im} \tilde{\psi}^{(1)}\left(x + \frac{\imath}{2}\right),$$

and

$$\lambda_m \frac{\partial T(\frac{1}{2}, y)}{\partial x} = \lambda_m \operatorname{Re} \left(\psi\left(\frac{1}{2} + \imath y\right) + B \right) = \lambda_m B_1 \left(\operatorname{Re} \left(\tilde{\psi}^{(1)}\left(\frac{1}{2} + \imath y\right) + 1 \right) \right).$$

Due to (41), integration on $[-\frac{1}{2}, \frac{1}{2}]$ the first equality gives

$$\lambda_m \int_{-\frac{1}{2}}^{\frac{1}{2}} \frac{\partial T(x, \frac{1}{2})}{\partial y} dx = 0.$$

Integrating on $[-\frac{1}{2}, \frac{1}{2}]$ the second equality and applying (11), we obtain the constant B_1 :

$$B_1 = \frac{-A \cos \theta}{\lambda_m(I + 1)}. \quad (42)$$

Similarly, taking $B_1 = 0$ (which corresponds to the problem (28)) and using (15), (18) and (38), we obtain

$$\lambda_m \frac{\partial T(x, \frac{1}{2})}{\partial y} = -\lambda_m \operatorname{Im} \left(\psi \left(x + \frac{i}{2} \right) + B \right) = -\lambda_m B_2 \operatorname{Im} \left(\tilde{\psi}^{(2)} \left(x + \frac{i}{2} \right) \right) - \lambda_m B_2,$$

and

$$\lambda_m \frac{\partial T(\frac{1}{2}, y)}{\partial x} = \lambda_m \operatorname{Re} \left(\psi \left(\frac{1}{2} + iy \right) + B \right) = \lambda_m B_2 \operatorname{Re} \left(\tilde{\psi}^{(2)} \left(\frac{1}{2} + iy \right) \right).$$

Using the equality $\tilde{\psi}^{(2)}(z) = -i\tilde{\psi}^\perp(-iz)$, we have

$$\operatorname{Im} \left(\tilde{\psi}^{(2)} \left(x + \frac{i}{2} \right) \right) = -\operatorname{Re} \left(\tilde{\psi}^\perp \left(\frac{1}{2} - ix \right) \right),$$

$$\operatorname{Re} \left(\tilde{\psi}^{(2)} \left(\frac{1}{2} + iy \right) \right) = \operatorname{Im} \left(\tilde{\psi}^\perp \left(-\frac{i}{2} + y \right) \right).$$

Thus, we get

$$\lambda_m \int_{-\frac{1}{2}}^{\frac{1}{2}} \frac{\partial T(\frac{1}{2}, y)}{\partial x} dy = 0.$$

Integrating on $[-\frac{1}{2}, \frac{1}{2}]$ the term $\lambda_m \frac{\partial T(x, \frac{1}{2})}{\partial y}$ and applying (10), we obtain the constant B_2 :

$$B_2 = \frac{-A \sin \theta}{\lambda_m(I^\perp - 1)}. \quad (43)$$

Taking into the account the properties of functions under consideration from Sections 2 and 3, the results obtained above and Remark 3.1, we arrive at the following theorem:

Theorem 4.1. *Let $T = T(x, y)$ and $T_k = T_k(x, y)$ be the solution of the problem (6)-(7), (10) and (11). The temperature flux is defined in the following form:*

$$\frac{\partial T(x, y)}{\partial x} - i \frac{\partial T(x, y)}{\partial y} = \begin{cases} \psi(z) + B, & z = x + iy \in D_{matrix}, \\ \frac{2\lambda_m}{\lambda_m + \lambda_k} \psi_k(z), & z = x + iy \in D_{inc}, \end{cases} \quad (44)$$

where

$$B = \frac{-A \cos \theta}{\lambda_m(I + 1)} - \frac{A \sin \theta}{\lambda_m(I^\perp - 1)} i,$$

and

$$\psi(z) := \frac{-A \cos \theta}{\lambda_m(I + 1)} \tilde{\psi}^{(1)}(z) + i \frac{A \sin \theta}{\lambda_m(I^\perp - 1)} \tilde{\psi}^\perp(-iz), \quad z \in D_{matrix},$$

$$\psi_k(z) := \frac{-A \cos \theta}{\lambda_m(I+1)} \tilde{\psi}_k^{(1)}(z) + \imath \frac{A \sin \theta}{\lambda_m(I^\perp - 1)} \tilde{\psi}_k^\perp(-\imath z), \quad z \in D_{inc}.$$

To find the temperature, it is sufficient to find the functions $\varphi, \varphi_1, \dots, \varphi_N$ (cf. (15)). These functions can be represented as sums $\varphi(z) = \varphi^{(1)}(z) + \varphi^{(2)}(z)$, $\varphi_k(z) = \varphi_k^{(1)}(z) + \varphi_k^{(2)}(z)$ of two functions $\varphi^{(1)}$ and $\varphi^{(2)}$ have to satisfy the following BVPs:

$$\varphi^{(1)}(t) = \varphi_k^{(1)}(t) - \overline{\rho_k \varphi_k^{(1)}(t)} - B_1 t, \quad (45)$$

$$\varphi^{(2)}(t) = \varphi_k^{(2)}(t) - \overline{\rho_k \varphi_k^{(2)}(t)} - \imath B_2 t. \quad (46)$$

Analogously to (38)–(39), we have $\varphi^{(1)}(z) = B_1 \tilde{\varphi}^{(1)}(z)$, $\varphi_k^{(1)}(z) = B_1 \tilde{\varphi}_k^{(1)}(z)$ and $\varphi^{(2)}(z) = B_2 \tilde{\varphi}^{(2)}(z)$, $\varphi_k^{(2)}(z) = B_2 \tilde{\varphi}_k^{(2)}(z)$. It is easy to verify that

$$\tilde{\varphi}^{(2)}(z) = \tilde{\varphi}^{(1)}(-\imath z), \quad \tilde{\varphi}_k^{(2)}(z) = \tilde{\varphi}_k^{(1)}(-\imath z).$$

The functions $\tilde{\varphi}^{(1)}$ and $\tilde{\varphi}_k^{(1)}$ can be found up to an arbitrary constant as indefinite integrals of the functions $\tilde{\psi}^{(1)}$ and $\tilde{\psi}_k^{(1)}$, respectively (cf. (35)). Thus, we arrive at the following statement:

Theorem 4.2. *Let $T = T(x, y)$ and $T_k = T_k(x, y)$ be the solution of the problem (6)–(7), (10) and (11). The temperature distribution can be found up to an arbitrary constant and is defined in the form (15), where*

$$B = \frac{-A \cos \theta}{\lambda_m(I+1)} - \frac{A \sin \theta}{\lambda_m(I^\perp - 1)} \imath,$$

$$\varphi(z) = \frac{-A \cos \theta}{\lambda_m(I+1)} \tilde{\varphi}^{(1)}(z) - \frac{A \sin \theta}{\lambda_m(I^\perp - 1)} \tilde{\varphi}^{(1)}(-\imath z),$$

$$\varphi_k(z) = \frac{-A \cos \theta}{\lambda_m(I+1)} \tilde{\varphi}_k^{(1)}(z) - \frac{A \sin \theta}{\lambda_m(I^\perp - 1)} \tilde{\varphi}_k^{(1)}(-\imath z).$$

Now we describe a new algorithm for solution of the problem (33). The problem (40) can be solved analogously. For convenience, we omit upper index in $\tilde{\psi}^{(1)}$ and will write $\tilde{\psi}$ below. We shortly describe solvability of the problem (33) using some facts and notation of the paper [1].

Notice that we have N contours ∂D_k and N complex conjugation conditions on each contour ∂D_k but we need to find $N+1$ functions $\tilde{\psi}, \tilde{\psi}_1, \dots, \tilde{\psi}_N$. This means that we need one additional condition to close up the system. For this reason we introduce a new doubly periodic function Φ which is a sectionally analytic in $Q_{(0,0)}$ and in $\bigcup_{k=1}^N D_k$ and has the zero jumps along each ∂D_k , $k = 1, 2, \dots, N$. Such consideration will give an additional condition on $\tilde{\psi}, \tilde{\psi}_1, \dots, \tilde{\psi}_N$. We will show that $\Phi \equiv 0$.

Let us introduce the sectionally analytic doubly periodic function Φ by the following formula:

$$\Phi(z) = \begin{cases} \tilde{\psi}_k(z) - \sum_{m=1}^N \rho_m \sum_{m_1, m_2}^* W_{m_1, m_2, m} \tilde{\psi}_m(z) - 1, & |z - a_k| \leq r_k, \\ \tilde{\psi}(z) - \sum_{m=1}^N \rho_m \sum_{m_1, m_2} W_{m_1, m_2, m} \tilde{\psi}_m(z), & z \in D_0, \end{cases} \quad (47)$$

where

$$W_{m_1, m_2, m} \tilde{\psi}_m(z) = \left(\frac{r_m}{z - a_m - m_1 - im_2} \right)^2 \overline{\tilde{\psi}_m \left(\frac{r_m^2}{z - a_m - m_1 - im_2} + a_m \right)} \quad (48)$$

and

$$\sum_{m=1}^N \sum_{m_1, m_2}^* W_{m_1, m_2, m} := \sum_{m \neq k} \sum_{m_1, m_2} W_{m_1, m_2, m} + \sum_{m_1, m_2}' W_{m_1, m_2, k}. \quad (49)$$

The ‘‘prime’’ notation in \sum_{m_1, m_2}' means that the summation occurs in all m_1 and m_2 except at $(m_1, m_2) = (0, 0)$.

Applying *Analytic Continuation Principle* and *Liouville’s* theorem for doubly periodic functions, we have that $\Phi = c$.

Let $\tilde{\psi}$ and $\tilde{\psi}_k$ be solutions of the system $\Phi(z) = c$. Then, in D_0 , we have

$$\tilde{\psi}(z) = \tilde{\psi}'(z) + c \quad (50)$$

with some doubly periodic function $\tilde{\psi}'$. Inserting the last equality in (35) and then in (30), we obtain

$$T(z) = \operatorname{Re}(\tilde{\varphi}'(z) + cz + z), \quad z \in D_0, \quad (51)$$

with some function $\tilde{\varphi}'$ which yields $c = 0$. Thus, we have $\Phi(z) \equiv 0$. Writing $\Phi(z) \equiv 0$, we obtain the following system of linear functional equations

$$\tilde{\psi}_k(z) = \sum_{m=1}^N \rho_m \sum_{m_1, m_2}^* W_{m_1, m_2, m} \tilde{\psi}_m(z) + 1 \quad (52)$$

which is uniquely solvable with respect to $\tilde{\psi}_k$ in the space of analytical functions (for more details cf. [1]).

The function $\tilde{\psi}$ has the form

$$\tilde{\psi}(z) = \sum_{m=1}^N \rho_m \sum_{m_1, m_2} W_{m_1, m_2, m} \tilde{\psi}_m(z). \quad (53)$$

Let us expand $\tilde{\psi}_k(z)$ into Taylor series

$$\tilde{\psi}_k(z) = \sum_{l=0}^{\infty} \tilde{\psi}_{lk}(z - a_k)^l \quad (54)$$

in order to sum up $W_{m_1, m_2, k} \tilde{\psi}_k(z)$ over all translations $m_1 + im_2$.

The series $\sum_j W_{j,k} \tilde{\psi}_k(z)$, where $j = (m_1, m_2)$ and k is a fixed number, can be represented via the elliptic Eisenstein functions $E_l(z)$ of order l (see [27]):

$$\sum_j W_{j,k} \tilde{\psi}_k(z) = \sum_{l=0}^{\infty} \overline{\tilde{\psi}_{lk} r_k^{2(l+1)}} E_{l+2}(z - a_k). \quad (55)$$

The series $\sum_j' W_{j,k} \tilde{\psi}_k(z) := \sum_j W_{j,k} \tilde{\psi}_k(z) - \left(\frac{r_k}{z-a_k}\right)^2 \overline{\tilde{\psi}_k \left(\frac{r_k^2}{z-a_k} + a_k\right)}$ can be written in the form

$$\sum_j' W_{j,k} \tilde{\psi}_k(z) = \sum_{l=0}^{\infty} \overline{\tilde{\psi}_{lk} r_k^{2(l+1)}} \sigma_{l+2}(z - a_k), \quad (56)$$

where σ_l is the modified Eisenstein function defined by the formula $\sigma_l(z) := E_l(z) - z^{-l}$. The Eisenstein functions E_l converges absolutely and uniformly for $l = 3, 4, \dots$ and conditionally for $l = 2$ ([27]).

Thus, we can rewrite the equations (52) and (53) for $\tilde{\psi}_k$ and $\tilde{\psi}$ as follows:

$$\tilde{\psi}_k(z) = \sum_{m \neq k}^N \sum_{l=0}^{\infty} \rho_m \overline{\tilde{\psi}_{lm} r_m^{2(l+1)}} E_{l+2}(z - a_m) + \sum_{l=0}^{\infty} \rho_k \overline{\tilde{\psi}_{lk} r_k^{2(l+1)}} \sigma_{l+2}(z - a_k) + 1, \quad (57)$$

$$\tilde{\psi}(z) = \sum_{m=1}^N \sum_{l=0}^{\infty} \rho_m \overline{\tilde{\psi}_{lm} r_m^{2(l+1)}} E_{l+2}(z - a_m). \quad (58)$$

Now we need to find the numerical coefficients $\tilde{\psi}_{lm}$ of the system (57). Note that the equation (58) for $\tilde{\psi}$ has the same coefficients $\tilde{\psi}_{lm}$. Taking a partial sum of Taylor series with M first items

$$\tilde{\psi}_k(z) = \tilde{\psi}_{0k} + \tilde{\psi}_{1k}(z - a_k) + \tilde{\psi}_{2k}(z - a_k)^2 + \dots + \tilde{\psi}_{Mk}(z - a_k)^M$$

and collecting the coefficients of the like powers of $z - a_k$, we obtain the formula for definition of $\tilde{\psi}_{jk}$:

$$\tilde{\psi}_{jk} = \frac{1}{j!} \tilde{\psi}_k^{(j)} \Big|_{z=a_k}, \quad (59)$$

where $\tilde{\psi}_k^{(j)}$ is derivative of order j of the function $\tilde{\psi}_k$. Then, we get

$$\begin{aligned} \tilde{\psi}_{jk} &= \frac{1}{j!} \sum_{m \neq k}^N \sum_{l=0}^M \rho_m \overline{\tilde{\psi}_{lm} r_m^{2(l+1)}} (-1)^j \frac{(l+j+1)!}{(l+1)!} E_{l+j+2}(a_k - a_m) \\ &+ \frac{1}{j!} \sum_{l=0}^M \rho_k \overline{\tilde{\psi}_{lk} r_k^{2(l+1)}} (-1)^j \frac{(l+j+1)!}{(l+1)!} \sigma_{l+j+2}(0) + I_j, \end{aligned} \quad (60)$$

where $I_j = \begin{cases} 1, & j = 0, \\ 0, & j = 1, \dots, M. \end{cases}$

Thus, we arrive at the system with $N(M+1)$ unknown constants $\tilde{\psi}_{jk}$ and $N(M+1)$ equations which can be solved numerically. Note that this system is obtained for an arbitrary number N of inclusions.

Remark 4.3. Note that doubly periodicity of E_{l+2} and the relations $E'_{l+2} = -(l+2)E_{l+3}$, $l = 0, 1, 2, \dots$ imply $\int_{-0.5}^{0.5} E_{l+2}(x + 0.5i) dx = 0$ for $l = 1, 2, \dots$, while

the equality $\int_{-0.5}^{0.5} E_2(x + 0.5i) dx = 0$ can be obtained by numerical calculation.

Therefore, $\int_{-0.5}^{0.5} \tilde{\psi}(x + 0.5i) dx = 0$.

Remark 4.4. Note that for finding of the flux distribution (namely, the functions $\tilde{\psi}, \tilde{\psi}_k, \dots, \tilde{\psi}_N$) in an explicit form, we change an algorithm of solution of the equations (57) and (58) in comparison with the algorithm represented in [1]. It allows to get more accurate numerical values of the flux in each point of considered composite material.

Remark 4.5. Note that it is possible to find the heat flux distribution in each cell $Q_{(m_1, m_2)}$ with corresponding centers $a_1 + m_1 + im_2, a_2 + m_1 + im_2, a_3 + m_1 + im_2, a_4 + m_1 + im_2$.

Thus in the next section when discussing numerical results we are concentrating only on the computations in the $Q_{(0,0)}$ unit cell.

5. Numerical results and discussions

5.1 The flux and the temperature distribution

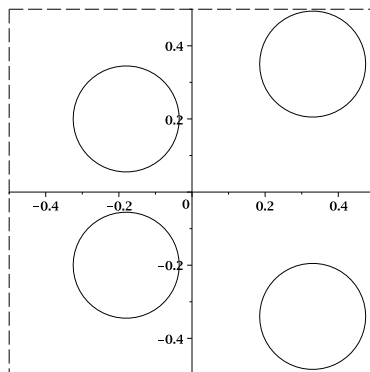
First we indirectly check the performance of the modified algorithm described in (57) – (60). As an example, we consider the case when four inclusions are situated within one cell, i.e., $N = 4$. We suppose throughout the computations that the heat flux of the fixed intensity $A = -1$ flows in different directions with respect to the main axis. Here the minus sign shows that the flux is directed from the right to the left (or from the top to the bottom) depending on the angle θ . The conductivity of the matrix is set as $\lambda_m = 1$, while those for the inclusions, λ_k , will take different values. The algorithm is realized in Maple 14 software.

We take for the first test a non-symmetrical configuration, with respect to Ox -axis, with two inclusions from the neighboring cells are situated very close to each other as depicted on Figure 2. The centers of the inclusions are situated in the points:

$$a_1 = -0.18 + 0.2i, \quad a_2 = 0.33 - 0.34i, \quad a_3 = 0.33 + 0.35i, \quad a_4 = -0.18 - 0.2i, \quad (61)$$

while their radii are the same $r_k = R$.

Convergence of the results computed for various numbers of the truncation parameter, M , showing how many terms are selected for computations in the Taylor series (54) is analyzed in the Table 1.

Figure 2. The cell $Q_{(0,0)}$.Table 1. The flux components for different truncation number M , while other problem parameters are: $\theta = 0$, $R = 0.145$, $\lambda_m = 1$, $\lambda_k = 100$ and the configurations of inclusion defined by (61).

M	$Q_x^{(1)}(a_1)$	$Q_y^{(1)}(a_1)$	$Q_x^{(m)}(0)$	$Q_y^{(m)}(0)$
0	1.50390574	-0.00595137	0.75430758	-0.00150794
1	1.51410894	-0.00549234	0.74026814	-0.00170226
2	1.51491054	-0.00568751	0.73098974	-0.00176024
3	1.51472013	-0.00569043	0.73081787	-0.00176227
4	1.51472348	-0.00569169	0.73081950	-0.00176386

The flux components Q_x and Q_y in the center a_k of k -inclusion

$$Q_x^{(k)}(a_k) \equiv \lambda_k \frac{\partial T_k(a_k)}{\partial x} = \frac{2\lambda_k \lambda_m}{\lambda_m + \lambda_k} \cdot \operatorname{Re} \psi_k(a_k),$$

$$Q_y^{(k)}(a_k) \equiv \lambda_k \frac{\partial T_k(a_k)}{\partial y} = -\frac{2\lambda_k \lambda_m}{\lambda_m + \lambda_k} \cdot \operatorname{Im} \psi_k(a_k),$$

are calculated in accordance with the formula (44). The flux components in any point of the matrix can be found as

$$Q_x^{(m)}(z) = \lambda_m \cdot \operatorname{Re}(\psi(z) + B), \quad Q_y^{(m)}(z) = -\lambda_m \cdot \operatorname{Im}(\psi(z) + B).$$

We calculate $Q_x^{(m)}(z)$ and $Q_y^{(m)}(z)$ at the point $z = 0 \in D_{matrix}$ belonging to the matrix. Computations in the Table 1 are given for four consequent value of the truncation number M ($M = 0, 1, \dots, 4$), and fixed other parameters: $\theta = 0$, $R = 0.145$, $\lambda_m = 1$, $\lambda_k = 100$.

Computations performed for this configuration and the material parameters suggest that, taking $M = 4$, the accuracy is between five or six valid units depending on where the flux is computed. Note that the material contrast is rather high thus the accuracy is good enough inside both the materials (in the matrix and in the inclusions). Clearly, the value of the inclusion radius affects the accuracy of the computations. Moreover, for symmetric configurations of the inclusions the accuracy is higher.

As an example, we also show the flux distribution inside the cell $Q_{(0,0)}$ for different angles and conductivities of inclusions on Figure 3-4. We take for calculations the centers of inclusions in the points (61) and the radius $R = 0.145$.

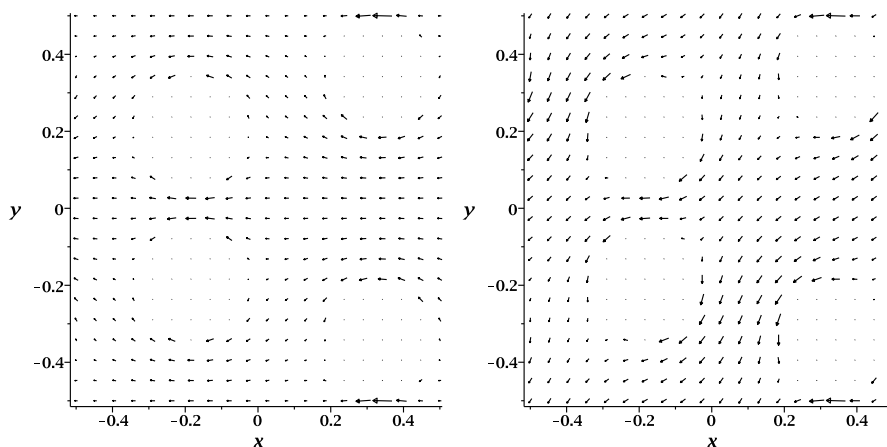


Figure 3. The flux distribution inside $Q_{(0,0)}$ for $\lambda_k = 0.01$, $\theta = 0; \pi/4$.

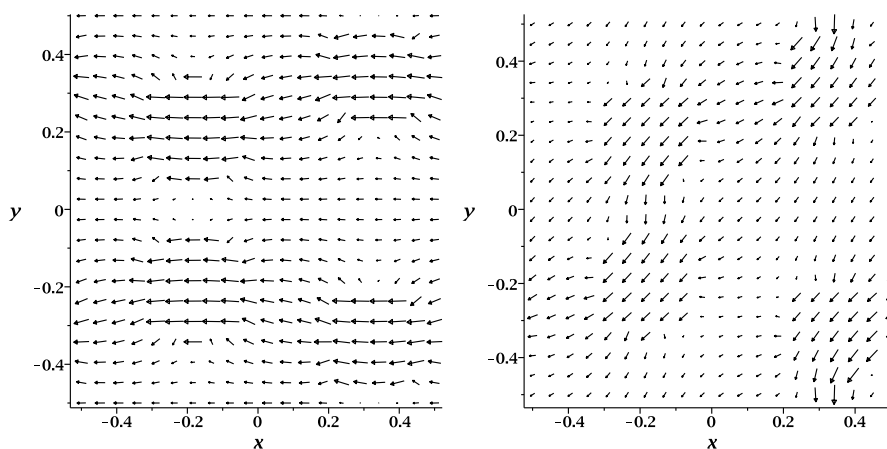


Figure 4. The flux distribution inside $Q_{(0,0)}$ for $\lambda_k = 100$, $\theta = 0; \pi/4$.

According to (15) in order to find the temperature function $T = T(x, y)$, one needs to find functions φ and φ_k , $k = 1, \dots, N$. Using (18) one can recover it, up to arbitrary constant, integrating functions ψ and ψ_k , $k = 1, \dots, N$. To define the constant, we use the boundary conditions (24). As a result of the integration, Weierstrass zeta-function appears (cf. Appendix A). The temperature distribution $T(x, y)$ is presented on Figure 5-6. The same two different contrast ratios (0.01 and 100) as for the flux distributions are given. Namely, we consider the following set of the parameters: $\lambda_m = 1$, $R = 0.145$, $\theta = 0; \frac{\pi}{4}$ with $\lambda_k = 100$ and $\lambda_k = 0.01$.

5.2 Average properties of the composite

The effective conductivity of microscopically isotropic composite materials with the inclusion volume fraction:

$$\nu = \sum_{k=1}^N \pi r_k^2 \ll 1$$

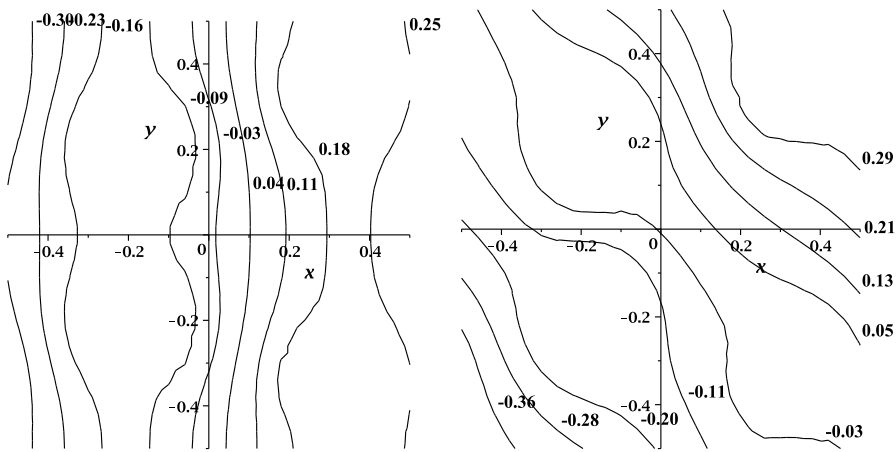


Figure 5. The temperature distribution inside $Q_{(0,0)}$ for $\lambda_k = 100$, $\theta = 0; \pi/4$.

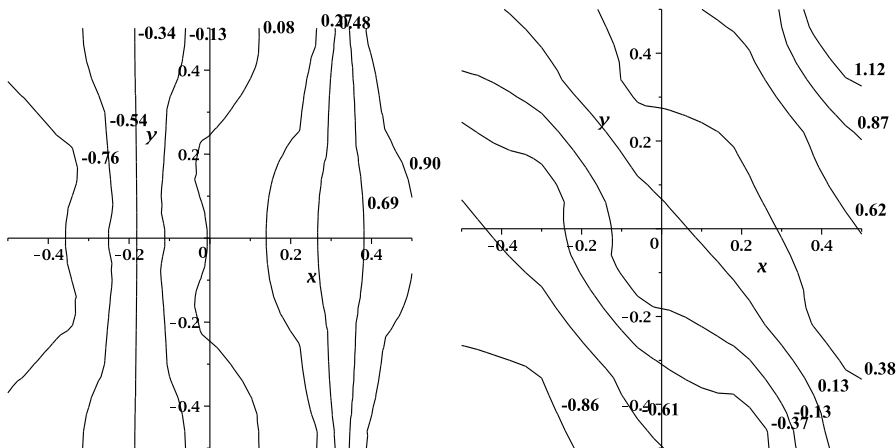


Figure 6. The temperature distribution inside $Q_{(0,0)}$ for $\lambda_k = 0.01$, $\theta = 0; \frac{\pi}{4}$.

is defined by the spherical tensor $\Lambda_e = \lambda_e \mathbf{I}$ where the effective conductivity is computed by the classical Maxwell formula

$$\lambda_e = \frac{1 + \rho\nu}{1 - \rho\nu} + \mathcal{O}(\nu^2), \quad \nu \rightarrow 0, \quad (62)$$

where $\lambda_m = 1$, $\rho = (\lambda_k - 1)/(\lambda_k + 1)$. For the history and applications of this formula see for example [28].

To compare the results obtained on the base of the improved algorithm and the classical Maxwell formula, we choose a periodic array of four inclusions ($N = 4$) placed symmetrically in the unit cell with the centers: $a_1 = -0.25 + 0.25i$, $a_2 = 0.25 + 0.25i$, $a_3 = 0.25 - 0.25i$, $a_4 = -0.25 - 0.25i$. Other parameters are: the flux flows along Ox -axis ($\theta = 0$), $A = -1$, inclusions conductivities $\lambda_k = 100$ and various values of the concentration parameter ν . In Table 2, a comparison of results calculated by two methods is presented. Here the value $\delta\lambda = (\lambda_e - \lambda_e^M)/\lambda_e$ indicates the accuracy of the approximate formula. We also supplement the computations by the results obtained using the FORTRAN code given in [15].

It is not a surprise that the results of the computations done for small inclusion

Table 2. Comparison of the effective conductivities: λ_e , λ_e^M and λ_e^* computed by the new algorithm, classic Maxwell formula and the algorithm presented in [15] for the symmetrically situated inclusions when $\lambda_m = 1$, $\lambda_k = 100$, $M = 4$.

R	ν	D/d	λ_e^M	λ_e	$\delta\lambda$	$\frac{\lambda_e - \lambda_e^M}{\nu^2}$	λ_e^*
0	0	0	1	1	0	—	1
0.005	0.00031	0.0204	1.00062	1.00062	$6.8 \cdot 10^{-19}$	$6.9 \cdot 10^{-12}$	1.00062
0.01	0.00126	0.0417	1.00247	1.00247	$1.8 \cdot 10^{-15}$	$1.1 \cdot 10^{-9}$	1.00247
0.03	0.01131	0.1364	1.02242	1.02242	$1.1 \cdot 10^{-10}$	$8.5 \cdot 10^{-7}$	1.02242
0.07	0.06158	0.3889	1.12847	1.12847	$5.1 \cdot 10^{-7}$	$1.5 \cdot 10^{-4}$	1.12848
0.1	0.12566	0.6667	1.28096	1.28098	$1.8 \cdot 10^{-5}$	$1.5 \cdot 10^{-3}$	1.28097
0.12	0.18095	0.9231	1.43123	1.43140	$1.6 \cdot 10^{-4}$	$5.0 \cdot 10^{-3}$	1.43138
0.145	0.26421	1.3810	1.69897	1.70032	$8.0 \cdot 10^{-4}$	$1.9 \cdot 10^{-2}$	1.70033
0.185	0.43008	2.8462	2.45762	2.48345	0.0104	0.1397	2.48342
0.2	0.50265	4.0	2.94245	3.01755	0.0249	0.2972	3.01742

Table 3. Comparison of the effective conductivities λ_e computed by the new algorithm and the classic Maxwell formula λ_e^M ($\lambda_m = 1$, $\lambda_k = 1/100$).

R	ν	D/d	λ_e^M	λ_e	$\delta\lambda$	$\frac{\lambda_e - \lambda_e^M}{\nu^2}$
0	0	0	1	1	0	—
0.005	0.00031	0.0204	0.99938	0.99938	$-2.4 \cdot 10^{-18}$	$-2.9 \cdot 10^{-11}$
0.01	0.00126	0.0417	0.99754	0.99754	$-1.8 \cdot 10^{-15}$	$-1.2 \cdot 10^{-9}$
0.03	0.01131	0.1364	0.97807	0.97807	$-1.1 \cdot 10^{-10}$	$-8.2 \cdot 10^{-7}$
0.07	0.06158	0.3889	0.88616	0.88616	$-5.1 \cdot 10^{-7}$	$-1.2 \cdot 10^{-4}$
0.1	0.12566	0.6667	0.78067	0.78065	$-1.8 \cdot 10^{-5}$	$-9.1 \cdot 10^{-4}$
0.12	0.18095	0.9231	0.69870	0.69862	$-1.6 \cdot 10^{-4}$	$-2.5 \cdot 10^{-3}$
0.145	0.26421	1.38095	0.58859	0.58812	$-8.0 \cdot 10^{-4}$	$-6.7 \cdot 10^{-3}$
0.185	0.43008	2.8462	0.40670	0.40267	-0.0105	-0.0229
0.2	0.50265	4.0	0.33985	0.33139	-0.0255	-0.0335

concentrations ($R = 0.005; 0.01; 0.03$) exhibit much better accuracy than that discussed in the Table 1. Here, $D = 2R$, d is a distance between inclusions giving an impression how far (close) to each other they are. On the contrary, the last two values of the volume fraction ν stand for rather high inclusion concentration. Our results confirm those obtained earlier (see, for example, [15, 25]) that the Maxwell formula provide a very good accuracy for a regular distribution of the inclusions up to the level of 30% in the volume fraction. As follows from the computations, to have the deviation between the formulas less than 1%, the distance between the inclusions should be larger than their diameters at least two times. Clearly, the results refer to the particular chosen configuration of inclusions, but interestingly does not much depend on the contrast parameter ρ .

From the results presented in the tables one could try to estimate the constants in the reminder $\mathcal{O}(\nu^2)$ from (62). However, the reminder in this particular case is rather of the order $\mathcal{O}(\nu^4)$. Clearly this should relate to the specific configuration of the inclusions in the composite. The authors failed to prove this or to find any known result supporting such a statement.

Finally, we estimate the accuracy of our computations by direct comparison with other known benchmarks. In the [29], the simplest geometry, one central inclusion was considered as one of the computational examples. Here, we present the respective data in the Table 4. In parentheses we also indicate the number of the terms in the Taylor series chosen by the authors to guarantee the desirable accuracy. We also compare our computations performed for $M = 4$ with those computed for the same number of iterations by the FORTRAN programme from [15]. For an additional check, we also present in the table the results computed for four symmetrical inclusions (which topologically and mechanically equivalent to the only central inclusions with the same volume fraction preserved). All the

Table 4. The effective conductivities λ_e computed by the new algorithm (for $M = 4$), the Perrins formula λ_e^P ([29]) (number of the terms is given in the parentheses), the classic Maxwell formula λ_e^M and the algorithm from [15] ($M = 5$) for $\lambda_m = 1$, $\lambda_k = 50$.

ν	$\lambda_e (N = 1)$	$\lambda_e (N = 4)$	$\lambda_e^P (M)$	λ_e^M	λ_e^*
0.1	1.21259	1.21259	1.2126 (1)	1.21258	1.21259
0.2	1.47599	1.47599	1.4760 (2)	1.47573	1.47599
0.3	1.81253	1.81253	1.8125 (2)	1.80992	1.81253
0.4	2.26325	2.26325	2.2633 (4)	2.24841	2.26325
0.5	2.91440	2.91447	2.9146 (4)	2.84906	2.91440
0.55	3.37256	3.37250	3.3732 (-)	3.24116	3.37256
0.6	3.98590	3.98653	3.9881 (8)	3.72222	3.98590

Table 5. The components of the effective conductivity tensor Λ_e for the configuration of the inclusions given in (61) for the material constants $\lambda_k = 100$, $\lambda_m = 1$, $M = 4$.

R	ν	λ_e^x	λ_e^{yx}	λ_e^y	λ_e^{xy}
0	0	1	0	1	0
0.05	0.03142	1.06285224	$2.434 \cdot 10^{-7}$	1.06425870	$2.434 \cdot 10^{-7}$
0.11	0.15205	1.331641	0.000008	1.375325	0.000008
0.135	0.22902	1.53413	0.000027	1.6630	0.000027
0.145	0.26421	1.6381	0.000047	1.844	0.000047

Table 6. The components of the effective conductivity tensor Λ_e for the configuration of the inclusions given in (61) for the material constants $\lambda_k = 1/100$ and $\lambda_m = 1$.

R	ν	λ_e^x	λ_e^{yx}	λ_e^y	λ_e^{xy}
0	0	1	0	1	0
0.05	0.03142	0.93962116	$2.152 \cdot 10^{-7}$	0.94086455	$2.152 \cdot 10^{-7}$
0.11	0.15205	0.727102	0.0000443	0.750954	0.0000443
0.135	0.22902	0.60148	0.000011	0.65186	0.000011
0.145	0.26421	0.5433	0.000016	0.611	0.000016

results are in a perfect agreement (taking into account the number of terms used in the computations of the Taylor series). Surprisingly, increasing number of the inclusions within the unit cell (preserving the composite topology), we achieved a slightly better results.

Now we return back to the original asymmetric configuration (61). The components λ_e^{ij} are calculated using the formula given in the Appendix B with use of the new algorithm. We present the computations for the materials conductivities $\lambda_m = 1$ and $\lambda_k = 100$; $1/100$. Values of all components of the tensor Λ_e as a function on the concentration ν are presented in Table 5 and in Table 6.

Thus the composite described by such configuration of the inclusions is not isotropic. The anisotropy increases with the value of the radius R (or, equivalently, with the volume fraction ν). The level of the computational accuracy in the Table 5 and Table 6 was controlled by a stabilization of the meaningful numbers.

To conclude the paper, we have proposed here the improved algorithm to solve the system (47). It allows us to reconstruct the solution and its gradient at an arbitrary point of the composite and the effective properties of the composite. We have shown an effectiveness of the improved algorithm on several examples and discussed peculiarities of the computations related to a particular configuration of the inclusions. And last but not least, the algorithm constructed in this paper may be used to compute practically arbitrary configurations of the inclusions in the composite using the benefits of the functional equation approach.

Acknowledgements

D. Kapanadze and E. Pesetskaya are supported by Shota Rustaveli National Science Foundation within grant FR/6/5-101/12 with the number 31/39. G. Mishuris is grateful to the FP7 PEOPLE IRSES Project TAMER under number 610547 for support of this research.

References

- [1] Berlyand L, Mityushev VV. Generalized Clausius–Mossotti formula for random composite with circular fibers. *J Stat Phys.* 2001;102:115–145.
- [2] King JL. A simple continuum model of a layered composite material. *J of Strain Analysis for Engineering Design.* 1972;7:146–150.
- [3] Markov KZ. Elementary Micromechanics of Heterogeneous Media. In *Heterogeneous Media: Modelling and Simulation.* Ed. by K.Z. Markov and L. Preziosi, Birkhauser Boston; 1999. p. 1-162.
- [4] Suen WM, Wong SP, Young K. The lattice model of heat conduction in a composite material. *J Phys D: Appl Phys.* 1979;12:1325–1338.
- [5] Allaire G. *Shape Optimization by the Homogenization Method.* Berlin, Springer Verlag; 2002.
- [6] Cherkhaev AV. *Variational Methods for Structural Optimization.* New York, Springer Verlag; 2000.
- [7] Kalamkarov AL, Kolpakov AG. *Analysis, Design and Optimization of Composite Structures.* Chichester, John Wiley & Sons; 1997.
- [8] Manevitch LI, Andrianov IV, Oshmyan VG. *Mechanics of Periodically Heterogeneous Structures.* Foundations of Engineering Mechanics, Berlin, Springer; 2002.
- [9] Milton GW. *The Theory of Composites.* Cambridge Monographs on Applied and Computational Mathematics. Cambridge University Press, Cambridge; 2002.
- [10] Movchan AV, Movchan NV, Poulton CG. *Asymptotic Models of Fields in Dilute and Densely Packed Composites.* London, Imperial College Press; 2002.
- [11] Bakhvalov NS, Panasenko GP. *Homogenization: Averaging Processes in Periodic Media.* Nauka, Moscow; 1984 (in Russian); English transl., Kluwer, Dordrecht/Boston/London; 1989.
- [12] Jikov VV, Kozlov SM, Oleinik OA. *Homogenization of Differential Operators and Integral Functionals.* Springer, Berlin; 1994.
- [13] Cherednichenko KD, Smyshlyaev VP. On full two-scale expansion of the solutions of nonlinear periodic rapidly oscillating problems and higher-order homogenised variational problems. *Arch Ration Mech Anal.* 2004;174:385–442.
- [14] Cherednichenko KD, Smyshlyaev VP, Zhikov VV. Non-local homogenized limits for composite media with highly anisotropic periodic fibres. *Proc R Soc Edin.* 2006;136:87–114.
- [15] Kushch VI. *Micromechanics of Composites: Multipole Expansion Approach.* Butterworth-Heinemann; 2013.
- [16] Mityushev V, Rogosin S. *Constructive Methods for Linear and Nonlinear Boundary Value Problems for Analytic Functions. Theory and Applications.* Monographs and Surveys in Pure and Applied Mathematics; 1999.
- [17] Obnosov YuV. *Boundary Value Problems of the Theory of Heterogeneous Media: Multiphase Media, Separated by Second Order Curves.* Kazan, Kazan State University [in Russian]; 2009.
- [18] Zohdi TI, Wriggers P. *Introduction to Computational Micromechanics.* Springer; 2005.
- [19] Andrianov IV, Bolshakov VI, Danishevskiy VV, Weichert D. Higher order asymptotic homogenization and wave propagation in periodic composite materials. *Proc R Soc London.* 2008;464:1181–1201.
- [20] Fiedler T, Pesetskaya E, Oechsner A, Grácio J. On the determination of the effective

- thermal conductivity of composite materials. Proceedings of the second Workshop on Advanced Computational Engineering Mechanics. Erlangen, Germany; 2005. p. 187–194.
- [21] Kachanov M, Tsukrov I, Shafiro B. Effective moduli of solids with cavities of various shapes. *Appl Mech Rev.* 1994;47:S151-S174.
- [22] Kanaun SK, Levin VM. *Self-Consistent Methods for Composites.* Springer; 2008.
- [23] Mityushev VV, Pesetskaya EV, Rogosin SV. Analytical methods for heat conduction in composites and porous media. *Thermal Properties of Cellular and Porous Materials.* Amsterdam, WILEY-VCH; 2007. p. 124–167.
- [24] Pesetskaya E. Effective conductivity of composite materials with random positions of cylindrical inclusions: finite number inclusions in the cell. *Applicable Analysis.* 2005;84:843–865.
- [25] Kachanov M, Sevostianov I. On quantitative characterization of microstructures and effective properties. *International Journal of Solids and Structures.* 2005;42:309-336.
- [26] Sevostianov I, Kachanov M. Connections between Elastic and Conductive Properties of Heterogeneous Materials. Ed. by H. Aref and E. van der Giessen. *Advances in Applied Mechanics.* 2008;42:69–252.
- [27] Weil A. *Elliptic Functions According to Eisenstein and Kronecker.* Springer-Verlag, Berlin; 1976.
- [28] Milton GW. *Mechanics of Composites.* Cambridge University Press, Cambridge; 2000.
- [29] Perrins WT, McKenzie DR, McPhedran RC. Transport Properties of Regular Arrays of Cylinders. *Proc R Soc Lond A.* 1979;369:207-225.
- [30] Hurwitz A. *Lectures on General Function Theory and Elliptic Functions.* (in German), Springer-Verlag, Berlin; 1964.

Appendix A. Description of the Eisenstein function of first order

This section contains the description of the Eisenstein function E_1 of first order. Properties of the Eisenstein functions of higher orders are described in details in [27].

The theory of elliptic functions provides the following formula for a lattice sum introduced by Rayleigh

$$S_{2n} := \sum'_{m_1, m_2} \frac{1}{(m_1 + im_2)^{2n}}.$$

The Eisenstein functions of order p are defines as

$$E_p(z) := \sum_{m_1, m_2} (z - m_1 - im_2)^{-p}.$$

The function E_2 and the Weierstrass function \wp are related by the identities ([30])

$$E_2(z) := \wp(z) + S_2,$$

where $S_2 = \pi$ for the square array.

The derivative of the Eisenstein function possesses the following property:

$$E'_p(z) = -p \cdot E_{p+1}(z).$$

Using this relation, we have $E_1'(z) = -E_2(z)$. Thus, integration on $[0, z]$ gives

$$E_1(z) = \zeta(z) - \pi z,$$

where ζ is the Weierstrass zeta function, and $\zeta'(z) = -\wp(z)$.

Appendix B. Evaluation of the effective conductivity

In general case of composites with different random non-overlapping inclusions the tensor of effective conductivity Λ_e has a form

$$\Lambda_e = \begin{pmatrix} \lambda_e^x & \lambda_e^{xy} \\ \lambda_e^{yx} & \lambda_e^y \end{pmatrix} \quad (\text{B1})$$

with components which can be found from the well-known equation

$$\langle \mathbf{q} \rangle = -\Lambda_e \cdot \langle \nabla T \rangle, \quad (\text{B2})$$

where $\langle \mathbf{q} \rangle = (\mathbf{q}_1, \mathbf{q}_2)$ is the average flux, and $\langle \nabla T \rangle = (T_1, T_2)$ is the average temperature gradient with

$$\mathbf{q}_j = \lambda_m \iint_{D_0} \frac{\partial T}{\partial x_j} dx_1 dx_2 + \sum_{k=1}^N \lambda_k \iint_{D_k} \frac{\partial T_k}{\partial x_j} dx_1 dx_2, \quad (\text{B3})$$

and

$$T_j = \iint_{D_0} \frac{\partial T}{\partial x_j} dx_1 dx_2 + \sum_{k=1}^N \iint_{D_k} \frac{\partial T_k}{\partial x_j} dx_1 dx_2, \quad (\text{B4})$$

where $j = 1, 2$ and $x_1 = x$ and $x_2 = y$.

The integrals above can be transformed using first Green's formula

$$\int_U (\psi \Delta \varphi + \nabla \varphi \cdot \nabla \psi) dV = \oint_{\partial U} \psi (\nabla \varphi \cdot \mathbf{n}) dS \quad (\text{B5})$$

with $\psi = x$ or $\psi = y$ and $\varphi(x, y) = T$ in D_0 (or $\varphi(x, y) = T_k$ in the respective domain D_k). Moreover,

$$\oint_{\partial D_0} x \frac{\partial T}{\partial n} ds = \oint_{\partial Q_{(0,0)}} x \frac{\partial T}{\partial n} ds - \sum_{k=1}^N \oint_{\partial D_k} x \frac{\partial T_k}{\partial n} ds, \quad (\text{B6})$$

where the curves $\partial Q_{(0,0)}$ and ∂D_k are oriented in the counterclockwise direction.

The first integral can be directly computed with use of (10), (11) and (12)

$$\oint_{\partial Q_{(0,0)}} x \frac{\partial T}{\partial n} ds = \int_{-1/2}^{1/2} x(-A \sin \theta) dx - \int_{-1/2}^{1/2} x(-A \sin \theta) dx +$$

$$\frac{1}{2} \int_{-1/2}^{1/2} (-A \cos \theta) dy + \frac{1}{2} \int_{-1/2}^{1/2} (-A \cos \theta) dy = -\frac{A}{\lambda_m} \cos \theta.$$

Repeating the same line of the reasoning with $\psi = y$ and $\varphi(x, y) = T$ in D_0 (or $\varphi(x, y) = T_k$ in the respective domain D_k) with first Green's formula (B5)

$$\oint_{\partial Q_{(0,0)}} y \frac{\partial T}{\partial n} ds = -\frac{A}{\lambda_m} \sin \theta. \quad (\text{B7})$$

Thus using the Green formula (B5), we have

$$\mathfrak{q}_1 = \lambda_m \left(\oint_{\partial Q_{(0,0)}} x \frac{\partial T}{\partial n} ds - \frac{\lambda_k}{\lambda_m} \sum_{k=1}^N \oint_{\partial D_k} x \frac{\partial T_k}{\partial n} ds \right) + \sum_{k=1}^N \lambda_k \oint_{\partial D_k} x \frac{\partial T_k}{\partial n} ds.$$

Using the fact that the contour integrals annihilate each other along the common boundaries ∂D_k and the formula (8), we finally obtain:

$$\mathfrak{q}_1 = \lambda_m \oint_{\partial Q_{(0,0)}} x \frac{\partial T}{\partial n} ds = -A \cos \theta.$$

Analogously,

$$\mathfrak{q}_2 = -A \sin \theta.$$

According to the same arguments as above, we have

$$T_1 = -\frac{A \cos \theta}{\lambda_m} + \sum_{k=1}^N \left(1 - \frac{\lambda_k}{\lambda_m}\right) \oint_{\partial D_k} x \frac{\partial T_k}{\partial n} ds = -\frac{A \cos \theta}{\lambda_m} + \sum_{k=1}^N \left(1 - \frac{\lambda_k}{\lambda_m}\right) \iint_{D_k} \frac{\partial T_k}{\partial x} dx dy,$$

$$T_2 = -\frac{A \sin \theta}{\lambda_m} + \sum_{k=1}^N \left(1 - \frac{\lambda_k}{\lambda_m}\right) \iint_{D_k} \frac{\partial T_k}{\partial y} dx dy.$$

Combining these values together with use of (18) and the mean value theorem for harmonic functions, we have

$$T_1 - iT_2 = \frac{-Ae^{-i\theta}}{\lambda_m} + 2 \sum_{k=1}^N \frac{\lambda_m - \lambda_k}{\lambda_m + \lambda_k} \iint_{D_k} \psi_k(z) dx dy = \frac{-Ae^{-i\theta}}{\lambda_m} - 2\pi \sum_{k=1}^N \rho_k r_k^2 \psi_k(a_k).$$